Homoclinic Snaking in a Semiconductor-Based Optical System

S. Barbay,* X. Hachair,† T. Elsass, I. Sagnes, and R. Kuszelewicz

Laboratoire de Photonique et de Nanostructures, CNRS, Route de Nozay, 91460 Marcoussis, France

(Received 16 June 2008; published 18 December 2008)

We report on experimental observations of homoclinic snaking in a vertical-cavity semiconductor optical amplifier. Our observations in a quasi-one-dimensional and two-dimensional configurations agree qualitatively well with what is expected from recent theoretical and numerical studies. In particular, we show the bifurcation sequence leading to a snaking bifurcation diagram linking single localized states to ''localized patterns'' or clusters of localized states and demonstrate a parameter region where cluster states are inhibited.

DOI: 10.1103/PhysRevLett.101.253902 PACS numbers: 42.65.Pc, 42.60.Da, 42.65.Tg, 89.75.Kd

Localized structures (LSs) in nonlinear extended systems are currently drawing a lot of attention from both theoretical and experimental points of view. This interest stems from the fact that, on the one hand, they represent promising objects in view of all-optical processing of information (in particular, in semiconductor-based optical systems [1–3]), and, on the other hand, the complete understanding of their properties and mechanism of formation is still the subject of interesting new developments [4,5]. LSs have been experimentally demonstrated in many systems besides semiconductor-based ones, e.g., in photorefractive oscillators [6], a liquid crystal light valve with feedback [7,8], magnetic fluids [9], a laser with a saturable absorber [10], gas discharge systems [11], and a sodium vapor with a single feedback mirror [12]. However, in view of applications, semiconductor-based systems are the most promising ones given the fast time scales (nanosecond range) and small space scales (microns) at stake. They usually appear as stationary bright spots sitting on a dark background that can be created (written) or destroyed (erased) at any transverse location of the system. Once the system is chosen and the parameters are fixed, LSs form a zero-parameter family of solutions having fixed shape and transverse dimensions; hence, they are called cavity solitons (CSs) in systems consisting of a nonlinear optical cavity. LSs can also be found in clusters or ''molecules'' [12,13]: At long distances LSs are independent of each other and form decorrelated objects, while at short distances they can interact to form bound states composed of several localized states. The relative stability of these states has been theoretically investigated in an optical system in [14]. The usual scenario [15,16] for the formation of LSs and clusters relies on the existence of a parameter range in which all of the multiplet LS states coexist. In the parameter range where a patterned state coexists with a uniform state, fronts connecting the uniform solution to the patterned state and back (homoclinic orbits) can form stable multiplet states. If there are two patterned states, multistability between two kinds of LSs can be observed [17]. In 1D, when a parameter is varied, the multiplet states lie on two oscillating curves (homoclinic snaking curve) with unstable and stable portions sharing a common parameter range, each representing the appearance of an odd or even number of solitary structures (see, e.g., [18]). On each stable branch, new structures are formed by symmetric addition of two lobes at each end of a multiplet state. This process reproduces itself until the upper branch, where periodic patterns are found, is reached or when the cluster state extends to the system's boundaries. The subcritical nature of the bifurcation that governs the appearance of the multiplet states makes it necessary to excite locally the system for the LS appearance and selection.

However, this theory says nothing in general about the kind of structure that emerges in 2D when several LSs are formed. A theoretical and numerical analysis in a nonlinear Kerr cavity revealed, however, the shape and stability of the few first clusters [14,19], and some experimental observations of clusters multistability in different systems were reported [11,20] without any clear reference or discussion in this theoretical context [21]. Experimentally, LSs can form either spontaneously by sweeping a parameter or by direct local addressing with an external perturbation. The former observation can be understood by including a global coupling term in the governing equations [4]. As a result, the homoclinic snaking curve describing LS formation is tilted, giving rise to the possibility of spontaneously generating single and higher-order localized states just by sweeping a parameter. These theories shed some light on the relationship between single localized spots and large patterns. This has also important consequences on possible applications to all-optical information processing: As an example, in the context of building a shift register line with trains of LSs (as in [22]) representing bits of information and where the independence of each bit is of prime importance, cluster-state formation is highly undesirable and needs to be thoroughly mastered.

In this Letter, we present and discuss experimental observations in quasi-1D and 2D configurations of homoclinic snaking in a vertical-cavity semiconductor optical amplifier. The homoclinic snaking bifurcation scenario for the cluster buildup is evidenced and is compared to theo-

retical predictions available mainly in 1D. Interesting consequences follow regarding the potential applications of semiconductor-based system for all-optical information processing.

Our experimental setup is shown in Fig. 1 and is similar to the one presented in [2,23]. It consists in a vertical-cavity semiconductor optical amplifier (VCSOA), specially designed for optical pumping [24] and injected by a holding beam (HB). The VCSOA microcavity was grown by metal-organic chemical vapor deposition with alternating AlGaAs/GaAs layers giving nominal 0.99 and 0.96 back and front mirrors reflectivities. The active zone is composed of a 2λ-thick bulk GaAs layer. The sample is bonded on a SiC substrate, and a $\sim$450-μm-thick SiC plate is put onto its front mirror to obtain a large heat dissipation and to be able to operate at high pump intensities. The VCSOA temperature is tuned and regulated thanks to a Peltier cooler and a feedback loop. The pump beam is delivered by a high-power, fiber coupled, laser diode array emitting at 800 nm. The output facet of the multimode 800-μm-diameter fiber is imaged on the sample surface to a 80-μm-diameter disk. The pump excitation is then mostly uniform on this area and has a top-hat shape. The coherent injected beam (holding beam) delivered by a Ti:sapphire laser is cleaned by Fourier filtering through a pinhole, passes through a quarter-wave plate and a dichroic mirror, and is focused onto the sample with a much broader beam waist so as to produce a quasiuniform illumination. The maximum holding beam intensity available on the sample is of the order of 150 mW. The intensity reflected by the sample is then analyzed by a camera (Cam) and a 150 MHz bandwidth photodetector (PD). The same photodetector monitors also the pump beam intensity that can be set by an arbitrary waveform generator (SIGGEN). SIGGEN's output consists in a small amplitude ramp with a period of 900 ms on top of a larger constant bias. A 1 GHz bandwidth digital oscilloscope acquires the signals from the different detectors. The oscilloscope, the pump laser, and the camera are all synchronized by a trigger event sent by SIGGEN. The camera acquires 60 evenly spaced images during the whole pump ramp with a 500 μs acquisition time.

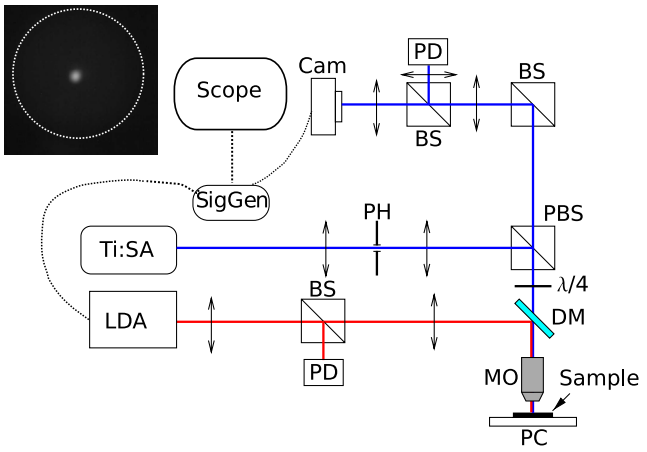

FIG. 1 (color online). Experimental setup. LDA: laser diode array; Ti:Sa: titanium-sapphire laser; PH: pinhole; PBS: polarizing beam splitter; BS: beam splitter; MO: 40× microscope objective; PC: Peltier cooler; PD: 150 MHz photodetector; Cam: fast digital camera and acquisition board; Scope: 1 GHz bandwidth digital oscilloscope; SIGGEN: arbitrary waveform generator. Dotted lines: Trigger events. Inset: Near-field image of a single CS. The dotted circle line marks the limits of the uniformly pumped area.

When the HB wavelength is slightly blue-detuned with respect to the cavity resonance, periodic patterns and localized structures can be found. A typical observation of a CS is shown on Fig. 1. We first introduce a slit in the experimental setup before the polarizing beam splitter such that its plane can be approximately imaged on the sample surface. This allows us to reproduce a quasi-one-dimensional system for which there exists a lot a theoretical work. The characteristic curve showing the total integrated reflected intensity versus pump power is shown in Fig. 2. The snapshots taken at different positions on this curve are shown in Fig. 3. The systems starts [Fig. 3(a)] in the stable plane-wave solution (uniform reflectivity) and then evolves towards the single-CS solution [Fig. 3(c)] when the pump power increases. These two states coexist with, respectively, a one- and a three-lobe state [Figs. 3(b) and 3(d)]. The switching from (c) to the upper branch where (d) lies is abrupt and is accompanied by the simultaneous and symmetric appearance of two side lobes as expected in 1D systems. The two-lobe state is not observed here. It can be due to the tilt present in the snaking curves (the branches for even and odd numbers of LSs are disconnected, and we may follow one branch without reaching the other one) or due to symmetry reasons that make the two-lobe state less stable than the odd-numbered lobe states. Indeed, the single CS state is preferably observed in the center of the system where all of the residual gradients present in the system tend to locate it. Note also that states (d) and (e) are similar, while state (f), though belonging to the same branch, develops additional lobes

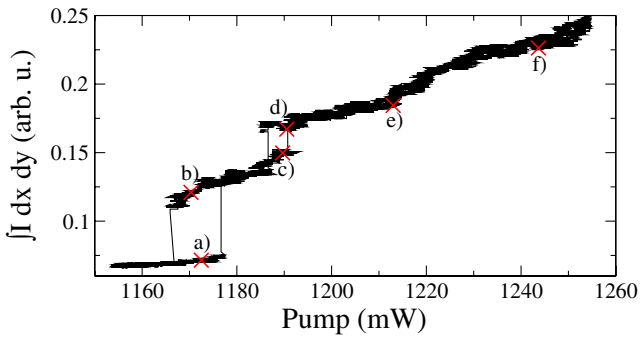

FIG. 2 (color online). Quasi-1D snaking curves obtained by varying the pump and recording both the images and the integrated reflected intensity. Red crosses mark the positions where snapshots have been taken.

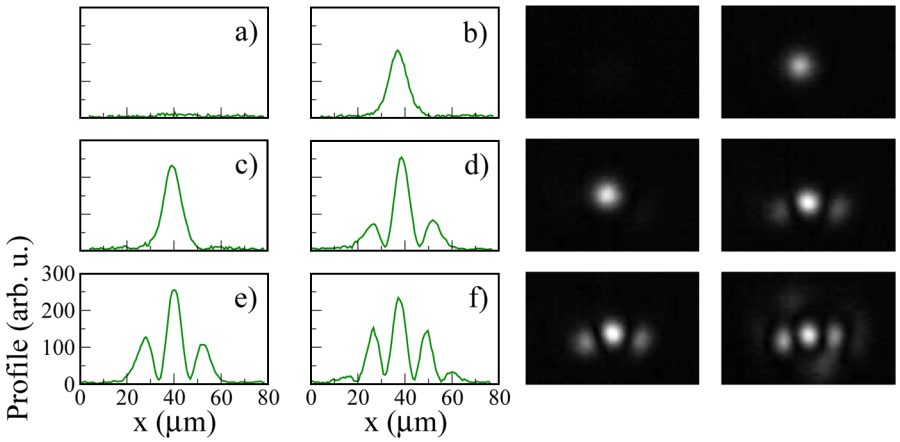

FIG. 3 (color online). Profiles and near-field images of the sample when the pump is varied as in Fig. 2.

without any abrupt transition. This may be the signature of the merge of the cluster states and the pattern branch. Since our system is not infinite in the transverse plane (and has physical constraints in one direction in this plane because of the presence of the slit), boundaries may influence the behavior of the cluster appearance and make the merging of the branches happen way before the appearance of very-high order cluster states [25]. An interesting feature of the higher-order soliton states is that the side lobes have amplitudes different from the central lobe and that the relative height of the side and central lobes varies appreciably on a given branch when the pump parameter changes. This can be understood when looking at the cluster structure as a combination of a rapidly oscillating spatial structure and an envelope, exponentially decreasing in the tails, in close connection to numerical results obtained in, e.g., [18].

An important tilt is present in the snaking curve which may here have several origins. One possible origin comes from the restriction of the system to develop in 1D because of the slit inserted in the HB path. Besides increasing the threshold for the multiple states to appear, the perturbation can be responsible for a tilt of the snaking curves. Another origin may come from a global coupling mechanism as shown in [14]. Although a thorough discussion of what this term might be in the physical situation of interest here is beyond the scope of this Letter, we mention local thermal effects due to different carrier densities as a possible mechanism. Indeed, where a localized state is present, the carrier density is locally depressed, and this should slightly decrease the temperature with a characteristic length dependent on the thermal diffusion of the sample. However, recent theoretical work suggests that this behavior is generic and can be explained in the framework of a local theory [21].

We remove the slit and the same experiment as above is repeated on the sample. Though the exact shape of the bifurcation and the selected clusters depends on the various experimental parameters that we may vary, typical results are shown in Fig. 4. In Fig. 4, the system starts from the uniform background, and a single CS and then higher-order LSs are shown. A four-lobe state appears now with side lobes almost evenly distributed around the central peak. The structure then grows by addition of three spots on a second ring, this large structure being bistable with the four-lobe structure and can be considered as a "localized pattern." When the pump is decreased, the hysteresis cycle is covered back passing through similar states. In such a system the snaking diagram is much more complex, and many more than two interleaved snaking curves are expected with respect to the 1D case. It is also interesting to note that in 2D, the two-lobe cluster state is not observed in this series of cluster states. However, we were able to record it with slightly different experimental parameters and on a different location of the sample as shown in Fig. 5(b). On each branch only the global intensity of the pattern changes, due to the pump parameter variation, but the appearance of an additional structure in the clusters is always abrupt. There are also small but noticeable orientation changes in the clusters belonging to the same branch

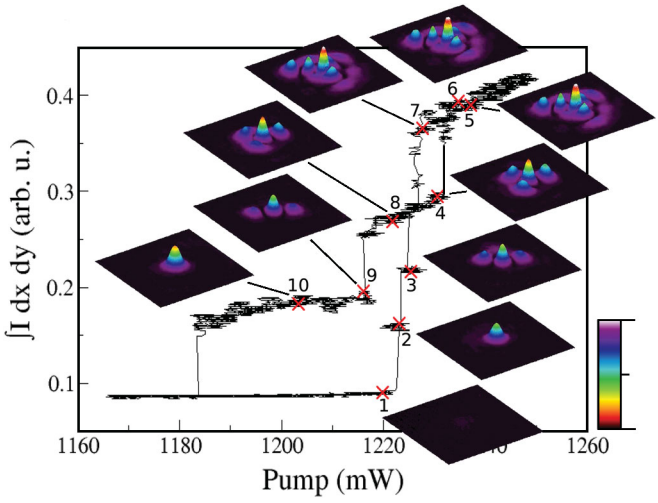

FIG. 4 (color). Bifurcation sequence of CS and clusters for $\lambda = 883.21$ nm. The near-field images recorded at given pump intensities are shown in false color and surface graphics. The numbers accompanying the images correspond to the order in which the images appear when the pump is ramped up and down. Image orientation is kept constant in the image processing.

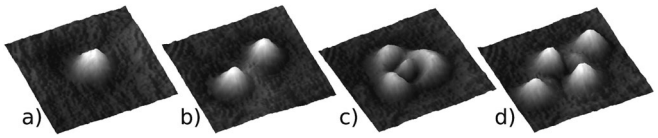

FIG. 5. Bifurcation sequence of a CS observed when ramping the pump for $\lambda = 884.62$ nm. The images are taken at pump powers: (a) 1276, (b) 1294, (c) 1307, and (d) 1329 mW. As in Fig. 4, partial multistability is observed between the four cluster states.

as clusters 3 and 9 or 4 and 8. In fact, approximately circularly symmetric cluster states are often observed in several orientations depending on the history of the system and on the noise that may induce configuration changes between these states having equal "total energy." It is also worthwhile noting that there exists a large pump intensity range where only the single-CS state can appear. This is in contrast with the simple picture of an infinite number of coexisting cluster states and may be related to the already mentioned tilt of the bifurcation diagram [4]. This is actually a very interesting point for applications since the appearance of cluster states may be considered a problem for applications requiring that a single CS state represent a fundamental bit of information.

Another possible bifurcation sequence is shown in Fig. 5. This sequence has been obtained without the front SiC plate and at a different wavelength, making the experimental conditions not exactly matched with the previous ones. On the sequence, two- and four-lobe states (in a rhomb shape) are observed.

Other types of cluster states, not showing a marked multistability as the two other examples shown before, are shown in Fig. 6. The interesting thing to notice is that most of these cluster states were theoretically predicted in Refs. [14,19]. The five-lobe cluster [Fig. 6(d)], the six-lobe cluster [Fig. 6(e)], and the hexagonal cluster [Fig. 6(f)] are all shown to be stable. The pentagonal cluster state with a central peak is shown to be unstable and has not been observed. The two-, three-, and four-lobe states [Figs. 5(b), 5(d), and 6(a)] were also found stable. In these models, a fast saturable absorption nonlinearity is used to model the nonlinear medium. This model is thus not perfectly adapted to our experimental conditions, but CSs are robust and generic objects found in many different types of nonlinearities, and it may be conjectured that the same holds for cluster states.

In conclusion, we have observed a homoclinic snaking bifurcation diagram in a vertical-cavity semiconductor optical amplifier. In the quasi-1D situation we are able to follow the buildup of the first cluster on the odd number of lobes branch in good agreement with theoretical predictions. In the 2D configuration, we show the complete bifurcation sequence and evidence a parameter range where the cluster states are inhibited.

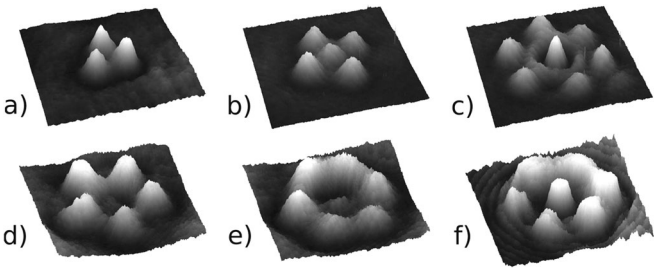

FIG. 6. Various isolated cluster states observed in similar experimental conditions as in Fig. 5.

This work has been carried out in the framework of the European project IST-STREP FunFACS (http://www.funfacs.org). We thank T. Ackemann for useful comments on the manuscript.

*sylvain.barbay@lpn.cnrs.fr; http://www.lpn.cnrs.fr
†Present address: INRIA, 2004 route des lucioles, B.P. 93, 06902 Sophia Antipolis, France.

[1] S. Barland *et al.*, Nature (London) **419**, 699 (2002).
[2] S. Barbay *et al.*, Opt. Lett. **31**, 1504 (2006).
[3] Y. Tanguy *et al.*, Phys. Rev. Lett. **100**, 013907 (2008).
[4] W. J. Firth, L. Columbo, and A. J. Scroggie, Phys. Rev. Lett. **99**, 104503 (2007).
[5] G. Kozyreff and S. J. Chapman, Phys. Rev. Lett. **97**, 044502 (2006).
[6] M. Saffman, D. Montgomery, and D. Z. Anderson, Opt. Lett. **19**, 518 (1994).
[7] R. Neubecker *et al.*, Phys. Rev. A **52**, 791 (1995).
[8] P. L. Ramazza *et al.*, J. Opt. B **2**, 399 (2000).
[9] R. Richter and I. V. Barashenkov, Phys. Rev. Lett. **94**, 184503 (2005).
[10] V. B. Taranenko, K. Staliunas, and C. O. Weiss, Phys. Rev. A **56**, 1582 (1997).
[11] Y. A. Astrov and Y. A. Logvin, Phys. Rev. Lett. **79**, 2983 (1997).
[12] B. Schäpers *et al.*, Phys. Rev. Lett. **85**, 748 (2000).
[13] Y. A. Astrov and H.-G. Purwins, Phys. Lett. A **283**, 349 (2001).
[14] A. G. Vladimirov *et al.*, Phys. Rev. E **65**, 046606 (2002).
[15] Y. Pomeau, Physica (Amsterdam) **23D**, 3 (1986).
[16] P. Coullet, C. Riera, and C. Tresser, Phys. Rev. Lett. **84**, 3069 (2000).
[17] U. Bortolozzo *et al.*, Phys. Rev. Lett. **93**, 253901 (2004).
[18] J. Burke and E. Knobloch, Phys. Rev. E **73**, 056211 (2006).
[19] J. M. McSloy *et al.*, Phys. Rev. E **66**, 046606 (2002).
[20] B. Schäpers, T. Ackemann, and W. Lange, IEEE J. Quantum Electron. **39**, 227 (2003).
[21] U. Bortolozzo, M. G. Clerc, and S. Residori, Phys. Rev. E **78**, 036214 (2008).
[22] F. Pedaci *et al.*, Appl. Phys. Lett. **92**, 011101 (2008).
[23] Y. Ménesguen *et al.*, Phys. Rev. A **74**, 023818 (2006).
[24] S. Barbay *et al.*, Appl. Phys. Lett. **86**, 151119 (2005).
[25] E. Knobloch, Nonlinearity **21**, T45 (2008).